Inorganic positive uniaxial films fabricated by serial bideposition

Ian Hodgkinson, Qi hong Wu, Lakshman De Silva and Matthew Arnold

Department of Physics, University of Otago, PO Box 56, Dunedin, New Zealand

ijh@physics.otago.ac.nz

Abstract: The physical vapor deposition process of serial bideposition is adapted to the fabrication of uniaxial optical coatings. During the coating process the vapor impinges at an angle of incidence of about 70° on to the substrate, and a stepwise axial rotation with 90° increments causes a columnar structure to grow normal to the substrate. Symmetry considerations that follow from the choice of 90° for the stepwise increment ensure that the film is achiral and has negligible in-plane linear birefringence. Optical characterization techniques confirm that films of tantalum oxide, titanium oxide and zirconium oxide are positive uniaxial with $n_e - n_o$ in the range 0.10 to 0.14.

OCIS codes: (160.1190) Anisotropic optical materials; (260.5430) Polarization; (260.1440) Birefringence; (310.6860) Thin films, optical properties; (310.1860) Deposition and fabrication; (310.1210) Coatings

References and links

1. I. J. Hodgkinson and Q. H. Wu, "Serial bideposition of anisotropic thin films with enhanced linear birefringence," Appl. Opt. **38** 3621–3625 (1999).
2. M. Born and E. Wolf, *Principles of Optics* (Pergamon Press, 1959).
3. P. Yeh and C. Gu, "Birefringent optical compensators for TN-LCDs," Proc. SPIE **3421**, 224-235 (1998).
4. J. P. Eblen, W. J. Gunning, D. B. Taber, P. Yeh, M. Khoshnevisan, J. Beedy, and L. G. Hale, "Thin-film birefringent devices based on form birefringence," Proc. SPIE **2262** 234-235 (1994).
5. K. Kaminska, T. Brown, G. Beydaghyan and K. Robbie, "Vacuum evaporated porous silicon photonic interference filters," Appl. Opt. **42**, 4212-4219 (2003).
6. J. M. Nieuwenhuizen, H. B. Haanstra, "Microfractography of thin films," Philips Tech. Rev. **27**, 87-91 (1966).
7. O. R. Monteiro, A. Vizir and I. G. Brown, "Multilayer thin-films with chevron-like microstructure," J. Phys. D: Appl. Phys. **31**, 3188-3196 (1998).
8. H. A. Macleod, *Thin film Optical Filters* (Adam Hilger 1969).
9. I. J. Hodgkinson and Q.H. Wu, *Birefringent Thin Films and Polarizing Elements* (World Scientific 1998).
10. I. J. Hodgkinson and Q. H. Wu, "Inorganic chiral optical materials," Adv. Mat. **13**, 889-897 (2001).

1. Introduction

Several imaging devices currently under development, including home theatre front projectors and rear projection digital televisions, require retarders that do not degrade under elevated temperatures and intense illumination. A possible solution is to use inorganic polarizing materials [1] which can be grown by physical vapor deposition (PVD). It is well known that a stack of thin films with alternating high and low refractive indices exhibits form (shape) birefringence and behaves like a uniaxial crystal [2]. By symmetry the optic axis is perpendicular to the planar

#4592 - $15.00 US
Received 10 June 2004; Revised 29 July 2004; accepted 29 July 2004

layers and light traveling along the optic axis does not cause depolarizing fields. As a consequence the ordinary index n_o is larger than the extraordinary index n_e, and by convention the multilayered material is said to be negative uniaxial. Such negative uniaxial materials can be fabricated by PVD of inorganic materials giving them, relative to organic polarizing materials, superiour physical and optical properties.

Yeh and Gu [3] have discussed the use of birefringent compensators for improving the viewing angle characteristics and gray scale stability of twisted nematic liquid crystal displays. Negative uniaxial, positive uniaxial, and biaxial films were all shown to play a useful role. Inorganic negative uniaxial films were fabricated for compensators by depositing alternating thin layers (20 nm thick) of silicon oxide and titanium oxide [4]. However, the sign of the birefringence of a planar layered structure is always negative, and hence a different approach is needed for the deposition of positive uniaxial films.

Thin films deposited at normal incidence tend to develop a normal-columnar nanostructure. The smallest depolarizing effects are along the columns and hence many thin films are intrinsically positive uniaxial. However additional nanoengineering is necessary in order to maximize the birefringence and to exercise control over the average refractive index. Recently Kaminska et. al. [5] reported a value of $n_e - n_o = 0.31$ and an average index of 2.13 for silicon deposited at 70° on to a rotating substrate and measured at $\lambda = 1000$ nm. Here we describe application of the serial bideposition (SBD) technique [1] to the growth of positive uniaxial films. We begin by reviewing the anisotropic nanostructures that have been produced by SBD, move on to outline methods for optical characterization of birefringent films, and conclude the article by presenting results for three materials.

2. Nanostructures formed by serial bideposition

In the SBD process that is illustrated schematically in Fig. 1 vapor that is incident on a substrate at angle θ_v tends to form a columnar nanostructure. If such a nanostructure is allowed to develop then the columns grow in the deposition plane at an angle ψ to the normal that is somewhat smaller than the deposition angle θ_v [6]. From an optical viewpoint the film is biaxial, rather like an orthorhombic crystal. We define the principal axes and principal refractive indices with n_1 corresponding to the direction of the columns, n_2 to the direction that is in the deposition plane and perpendicular to the columns, and n_3 to the direction perpendicular to the deposition plane. For the materials that we have studied the principal refractive indices satisfy $n_1 > n_3 > n_2$, and for light at normal incidence the effective combination n_p of n_1 and n_2 is found to be smaller than n_3. Thus the effective birefringence $\Delta n = n_3 - n_p$ of the materials is positive.

Such a tilted-columnar biaxial film is one option, albeit trivial, for SBD. However, a more common target of SBD is modification of columnar growth, and this can be achieved through stepwise rotations of the substrate about its normal. Here we consider the most basic case in which rotations by a constant angle $\Delta\xi$ are made repeatedly and under computer control following each deposition of a constant preset increment Δd of material.

When Δd is typically a few nanometers the deposition conditions are such that chevron layers [7] are unable to form, and instead a new columnar structure develops. As an example, with $\Delta\xi = 180^\circ$ the new columnar nanostructure runs perpendicular to the substrate and the normal-incidence birefringence $n_3 - n_2$ can exceed Δn for a tilted-columnar film by a factor of 2. With the same value of Δd and a small angular increment, typically about 4°, a chiral (handed) nanostructure like a single-start screw grows whereas adopting an angular increment of $\Delta\xi = 184^\circ$ leads to a double-start screw form. Table 1 provides a summary of these nanostructures. Significantly for our study, a film will be achiral only for the cases with $\Delta\xi = 0^\circ$, 90° or 180°.

In this article we shall confirm that an angular increment of 90° combined with small values of Δd leads to a normal-columnar uniaxial nanostructure. Given that the axis is normal to the

#4592 - $15.00 US Received 10 June 2004; Revised 29 July 2004; accepted 29 July 2004

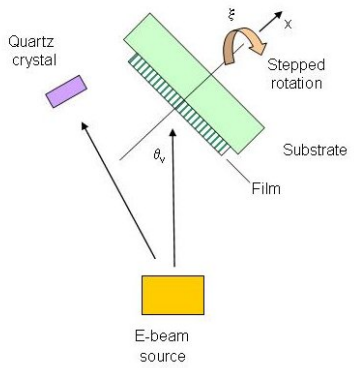

Fig. 1. Coating setup for serial bideposition.

substrate we can replace n_1 with the extraordinary index n_e and n_2, n_3 with the ordinary index n_o. If as anticipated, n_e (along the columns) is greater than n_o (perpendicular to the columns), then we will have fabricated a positive uniaxial medium. In the following section we outline the methods that were used to characterize the new inorganic birefringent media.

Table 1. Nanostructures formed by serial bideposition.

Angular increment (degree)	Thin film nanostructure
0	tilted-columnar biaxial
≈ 4	single-helix chiral
90	normal-columnar uniaxial
180	normal-columnar biaxial
≈ 184	double-helix chiral

3. Optical characterization

We record angular retardance maps to verify the structural symmetry of the nanostructures that we fabricate using SBD. As this assessment is qualitative an additional method is needed for determining the values of n_o and n_e for the uniaxial films made for this study. In general we favor a method that does not rely on absolute measurements of reflectance or transmittance. As a first step in the procedure that we use an adaptation of the Abelès Brewster angle method [8] is used to provide an equation that connects n_o and n_e, and then an optimization method is used to fit material values to a retardance versus optical angle of incidence profile.

3.1. Angular retardance maps

By using the method of post-deposition characterization that is illustrated in Fig. 2 angular retardance maps can be recorded pixel by pixel for angles of incidence in the range $0^\circ \leq \theta \leq 35^\circ$ and for angles of rotation $0^\circ \leq \theta \leq 360^\circ$. Each map is a projection of retardance, plotted against axes $\beta \cos\xi$ (horizontal, corresponding to the deposition plane) and $\beta \sin\xi$. The parameter β is the Snell's law invariant.

#4592 - $15.00 US
Received 10 June 2004; Revised 29 July 2004; accepted 29 July 2004

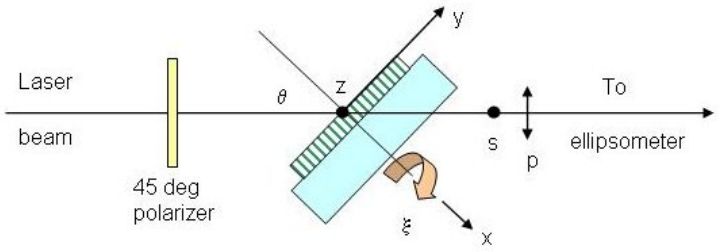

Fig. 2. Apparatus used for mapping angular retardance.

For comparison with the experimental maps, simulated maps are computed using a 4×4 matrix method [9] in which a biaxial layer is represented by three principal refractive indices and three angles η, ψ, ξ that specify the angular location of axes. Parameters used in these simulations are listed in Table 2.

Symmetry elements in a map indicate the structural form of the nanostructure. Thus the simulated and experimental maps (S1 and E1) shown in Fig. 3 for a normal-columnar biaxial nanostructure have two axes of symmetry. Similary the maps S2 and E2 for a tilted-columnar biaxial nanostructure have a single axis of symmetry, the maps S3+ and S3- for positive and negative normal-columnar uniaxial nanostructures are symmetric about a central point. For comparison we have included maps S4 and E4 for a film with all principal axes inclined to the surface of the substrate, as these maps do not have an axis of symmetry.

Table 2. Parameters used in simulations of angular retardance maps.

Simulation	n_1	n_2	n_3	η (rad)	ψ (rad)	ξ (rad)	d/λ
S1	2.0	1.7	1.84	0	0	0	2
S2	2.145	1.865	1.991	0	0.491	0	2
S3+	1.78	1.64	1.64	0	0	0	1.975
S3-	1.64	1.78	1.78	0	0	0	1.975
S4	1.95	1.635	1.722	-0.268	0.625	0.222	1.264

In Fig. 4 we display the symmetry elements that are exhibited by the maps in Fig. 3.

3.2. Abelès method for uniaxial films

In the Abelès Brewster angle method, which is illustrated in Fig. 5, the substrate is illuminated with *p*-polarized light and rotated so that the reflectance (or visual brightness) of the coated part matches the reflectance of the uncoated part. The optical angle of incidence is then the Brewster angle θ_B, and the Brewster index n_B which is the refractive index for an isotropic film is calulated using

$$n_B = \tan \theta_B. \tag{1}$$

The method has an important advantage, that the result does not depend on knowledge of the film thickness, and hence a potential error of $\pm 5\%$ or so is avoided.

Using the notation and appropriate equations from Ref. [9] we adapt Abelès method to uniaxial films. We note that the condition for equal reflectances from an uncoated substrate and a

#4592 - $15.00 US
Received 10 June 2004; Revised 29 July 2004; accepted 29 July 2004

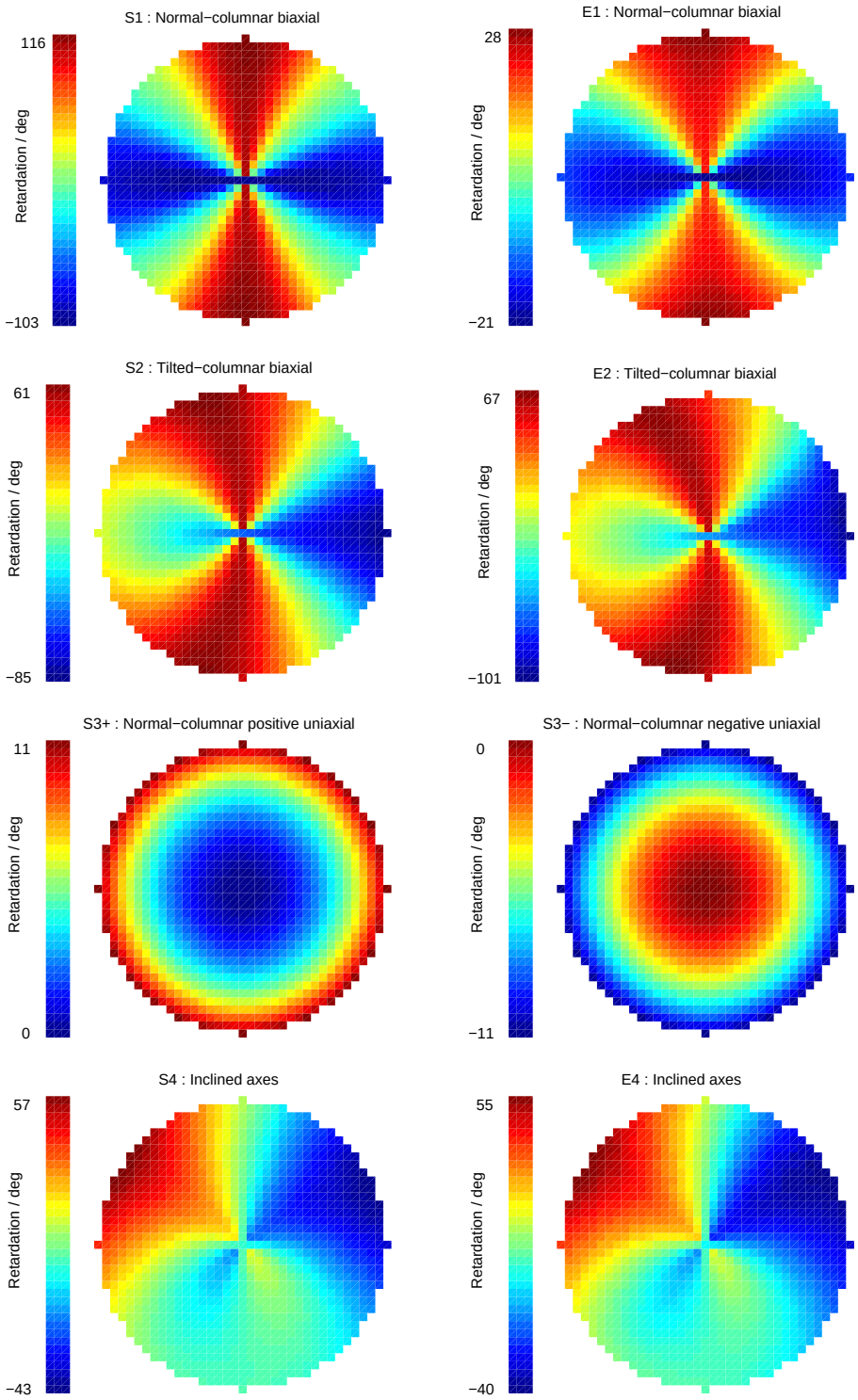

Fig. 3. (Top) Simulated and experimental angular retardance maps for a normal-columnar biaxial film; (upper-middle) simulated and experimental maps for a tilted-columnar biaxial film; (lower-middle) simulated maps for normal-columnar positive and negative uniaxial films; (bottom) simulated and experimental maps for a film with all principal axes inclined to the surface of the substrate.

#4592 - $15.00 US Received 10 June 2004; Revised 29 July 2004; accepted 29 July 2004

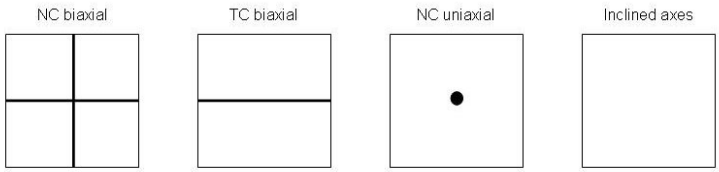

Fig. 4. Symmetries of angular retardance maps for normal-columnar biaxial, tilted-columnar biaxial, normal-columnar uniaxial nanostructures and for a film with all axes inclined to the surface of the substrate.

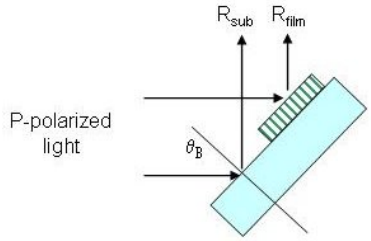

Fig. 5. Apparatus used for measuring the Abelès refractive index.

substrate coated with a unixial film can be stated as

$$\gamma_{film} = \gamma_{sub} \tag{2}$$

where $\gamma_{film} = 1/z_0(1/n_o^2 - \beta^2/n_o^2 n_e^2)^{1/2}$ and $\gamma_{sub} = 1/z_0(1-\beta^2)^{1/2}$ are, respectively, the field ratio parameters for the coated and uncoated substrate and here $\beta = \sin\theta_B$. The equation that follows,

$$n_B = n_e \left(\frac{n_e^2 - 1}{n_o^2 - 1} \right)^{1/2}, \tag{3}$$

provides a useful connection between n_o and n_e.

3.3. Angle-resolved retardance profiles

Typical calculations indicate that the profile of retardance Δ versus optical angle of incidence θ for a uniaxial film may contain strong modulations due to interference effects. Interference modulations are particulary strong when n_o and n_e are substantially different from the refractive index of the substrate. As shown in Fig. 6 the profile for a slab of bulk material (without interference effects) essentially runs through the middle of the modulated profile for the film with interference. In these simulations the uniaxial material was assumed to have an average index $(n_o + n_e)/2$ equal to 2 and thickness $d = 2\,\mu$m. The thin film calculations used the additional values:- cover index $n_C = 1.0$, substrate index $n_S = 1.516$ and wavelength $\lambda = 633\,$nm.

#4592 - $15.00 US
Received 10 June 2004; Revised 29 July 2004; accepted 29 July 2004

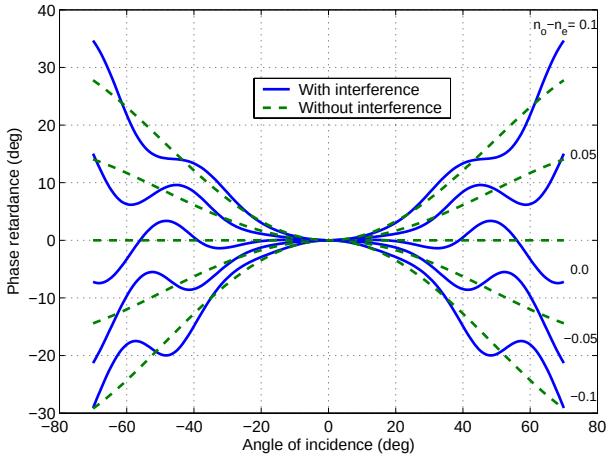

Fig. 6. Retardance profiles simulated for a 2-μm slab of a uniaxial material without interference, and for a film of the same material with interference.

We use an optimization program to fit a material-type profile to the experimental Δ versus θ data. In this procedure a value of n_o is selected and the corresponding n_e is calculated using Eq. (3). Then the bulk material profile that is required for the fitting procedure is computed using the equation

$$\Delta = 2\pi n_o d[(1-\beta^2/n_e^2)^{1/2} - (1-\beta^2/n_o^2)^{1/2}]/\lambda \tag{4}$$

which has been adapted from Ref. [9].

For this part we were obliged to use a film thickness substantially greater than the thickness of approximately one quarterwave that gives greatest sensitivity for the Brewster angle method. Specifically the experimental profile should have a few modulations and hence thicknesses of 1 μm or so were used.

4. Results

We report results for films of tantalum oxide, titanium oxide and zirconium oxide grown using SBD with 90° angular increments, as described above in Sect. 2. Typical deposition conditions included a backfill of oxygen, substrate temperature 300°C and a deposition rate of 1 nm/s. The tantalum oxide film received post-deposition heating in air to reduce absorption to an acceptable level.

Refractive indices measured for the three films using light of wavelength 633 nm are listed in Table 3. The substantial values of birefringence that were obtained (0.10–0.14) are comparable to the best normal-incidence values recorded for normal-columnar biaxial films. And, as in the case of the normal-columnar biaxial films, decreasing the deposition angle tends to lead to larger principal indices and smaller birefringence.

An angular retardance map (E5) recorded for the tantalum oxide film is reproduced in Fig. 7. This map exhibits the basic circular symmetry that is expected for a positive uniaxial film. As well a small asymmetry is revealed in E5 that can be used for estimation of the integrity of the uniaxial structure. After analysing simulations we concluded that the structure is not exactly uniaxial, rather than tilted-uniaxial say, and the in-plane birefringence $n_3 - n_2$ was estimated to be -0.0007. The corresponding simulation is S5 in Fig. 7.

#4592 - $15.00 US
Received 10 June 2004; Revised 29 July 2004; accepted 29 July 2004

Table 3. Properties of inorganic positive uniaxial films ($\lambda = 633$nm).

Oxide	Dep. angle	Thickness μm	Brewster index	Ordinary index	Extraord. index	Birefringence
	θ_v	d	n_B	n_e	n_o	$n_e - n_o$
Tantalum	70	1.25	1.57	1.78	1.64	0.14
Titanium	80	0.7	1.43	1.66	1.52	0.14
Zirconium	70	1.3	1.56	1.71	1.61	0.10

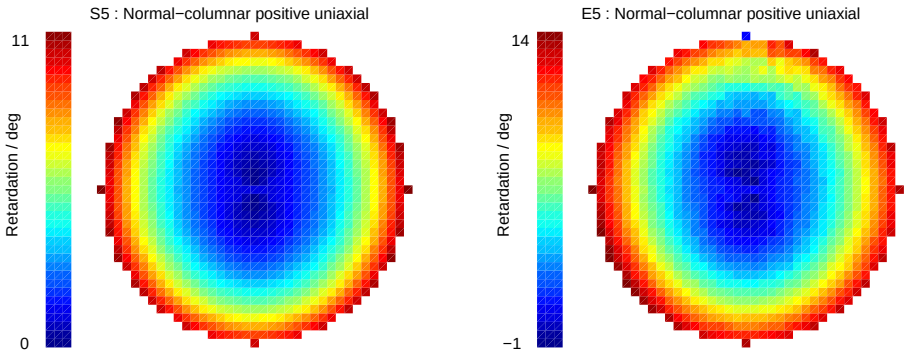

Fig. 7. Simulated and experimental angular retardance maps for a positive normal-columnar uniaxial film with a small in-plane anisotropy.

5. Summary

We have adapted the SBD technique to the fabrication of positive uniaxial thin film media. Repeated depositions of a few nanometers of material on to a tilted substrate that is rotated in angular increments of 90° leads to the growth of films with substantial values of $n_e - n_o$. Best results for materials designed for use at visible wavelengths were obtained for tantulum oxide and titanium oxide.

Acknowledgments

The authors acknowledge support from the New Zealand New Economy Research Fund and from the MacDiarmid Centre for Research Excellence.

#4592 - $15.00 US Received 10 June 2004; Revised 29 July 2004; accepted 29 July 2004